Monthly Notices of the ROYAL ASTRONOMICAL SOCIETY

MNRAS **452,** 24–31 (2015) doi:10.1093/mnras/stv1308

The evolution of a jet ejection of the ultraluminous X-ray source Holmberg II X-1

D. Cseh,[1⋆] J. C. A. Miller-Jones,[2] P. G. Jonker,[3,1] F. Grisé,[4] Z. Paragi,[5] S. Corbel,[6,7] H. Falcke,[1] S. Frey,[8] P. Kaaret[9] and E. Körding[1]

[1]*Department of Astrophysics/IMAPP, Radboud University Nijmegen, PO Box 9010, NL-6500 GL Nijmegen, the Netherlands*
[2]*International Centre for Radio Astronomy Research – Curtin University, GPO Box U1987, Perth, WA 6845, Australia*
[3]*SRON, Netherlands Institute for Space Research, Sorbonnelaan 2, NL-3584 CA Utrecht, the Netherlands*
[4]*Observatoire astronomique de Strasbourg, Université de Strasbourg, CNRS, UMR 7550, 11 rue de l'Université, F-67000 Strasbourg, France*
[5]*Joint Institute for VLBI in Europe, Postbus 2, NL-7990 AA Dwingeloo, the Netherlands*
[6]*Laboratoire AIM (CEA/IRFU-CNRS/INSU-Université Paris Diderot), CEA/DSM/IRFU/SAp, F-91191 Gif-sur-Yvette, France*
[7]*Station de Radioastronomie de Nançay, Observatoire de Paris, CNRS/INSU, USR 704 – Univ. Orléans, OSUC, F-18330 Nançay, France*
[8]*FÖMI Satellite Geodetic Observatory, PO Box 585, H-1592 Budapest, Hungary*
[9]*Department of Physics and Astronomy, University of Iowa, Iowa City, IA 52240, USA*

Accepted 2015 June 8. Received 2015 June 2; in original form 2015 April 24

ABSTRACT

We present quasi-simultaneous, multi-epoch radio and X-ray measurements of Holmberg II X-1 using the European VLBI Network (EVN), the Karl G. Jansky Very Large Array (VLA), and the *Chandra* and *Swift* X-ray telescopes. The X-ray data show apparently hard spectra with steady X-ray luminosities four months apart from each other. In the high-resolution EVN radio observations, we have detected an extended milliarcsecond scale source with unboosted radio emission. The source emits non-thermal, likely optically thin synchrotron emission, and its morphology is consistent with a jet ejection. The 9-GHz VLA data show an arcsecond-scale triple structure of Holmberg II X-1 similar to that seen at lower frequencies. However, we find that the central ejection has faded by at least a factor of 7.3 over 1.5 yr. We estimate the dynamical age of the ejection to be higher than 2.1 yr. We show that such a rapid cooling can be explained with simple adiabatic expansion losses. These properties of Holmberg II X-1 imply that ULX radio bubbles may be inflated by ejecta instead of self-absorbed compact jets.

Key words: accretion, accretion discs – black hole physics – X-rays: binaries.

1 INTRODUCTION

Ultraluminous X-ray sources (ULXs) host accreting compact objects, whose luminosity ($L_X > 3 \times 10^{39}$ erg s^{-1}) exceeds the Eddington limit of a 20-M$_\odot$ black hole (BH). ULXs are a mixed bag of sources. Some may host super-Eddington neutron stars (Bachetti et al. 2014) or stellar-mass ($M = 3$–20 M$_\odot$) BHs (Liu et al. 2013; Motch et al. 2014). Some of them are likely to be intermediate-mass $M = 10^2$–10^5 M$_\odot$ BHs (Farrell et al. 2009; Feng & Kaaret 2010; Pasham, Strohmayer & Mushotzky 2014; Mezcua et al. 2015) and may also host recoiling supermassive BHs (Jonker et al. 2010).

Given the tentative observational evidence for the anticorrelation between BH mass and host galaxy metallicity (Crowther et al. 2010) and that some ULX progenitor stars could potentially have been massive enough (e.g. Grisé et al. 2012; Poutanen et al. 2013) to collapse directly to a BH, ULXs might host massive stellar mass (20–100 M$_\odot$) BHs (Fryer 1999; Mapelli, Colpi & Zampieri 2009; Zampieri & Roberts 2009; Belczynski et al. 2010; Bachetti et al. 2013; Mapelli & Bressan 2013). In fact, Holmberg II X-1 lies in a relatively metal-poor dwarf irregular galaxy (Prestwich et al. 2013; Brorby, Kaaret & Feng 2015). Such a mass range has been shown to fit its observed X-ray and radio properties (Goad et al. 2006; Cseh et al. 2014) and may also be valid for IC 342 X-1 (Marlowe et al. 2014).

To date, relatively few ULX radio counterparts have been studied, and these few show a relatively diverse nature. The first radio bubble, associated with NGC 5408 X-1, was discovered about a decade ago (Kaaret et al. 2003) although one other, associated with NGC 6946 X-1, was detected earlier but considered as a super- or hypernova remnant (van Dyk et al. 1994). Following the discoveries of more radio bubbles (e.g. Cseh et al. 2012, and references therein), transient jets were also caught in two non-persistent ULXs, which in both cases were associated with X-ray outbursts of the central compact object (Webb et al. 2012; Middleton et al. 2013). Furthermore, in a few other cases, apparently steady radio emission has

⋆ E-mail: d.cseh@astro.ru.nl

been detected on milliarcsecond scales (Mezcua & Lobanov 2011; Mezcua et al. 2013, 2015) and interpreted as self-absorbed radio cores, which are typically seen during radiatively inefficient accretion states of Galactic BH X-ray binaries (e.g. Fender, Homan & Belloni 2009).

Focusing on the large-scale environments of ULXs, jets have been argued to be a plausible supply mechanism responsible for inflating the observed radio bubbles (and shock-ionized optical bubbles e.g. Cseh et al. 2012). On the other hand, direct evidence of jets in Holmberg II X-1 (Cseh et al. 2014) has been found, despite an environment that appears to be dominated by photoionization (Lehmann et al. 2005; Egorov, Lozinskaya & Moiseev 2013). This may indicate that shock ionization is not a necessary consequence of jets. Shock-ionized optical bubbles (e.g. Pakull & Mirioni 2002; Pakull & Grisé 2008) could equally be inflated by powerful winds. These winds are thought to originate from a supercritical disc that may also give rise to geometrically collimated X-rays (Poutanen et al. 2007) although calorimetry of photoionized optical bubbles argues against strongly beamed X-ray emission (e.g. Pakull & Mirioni 2002; Kaaret & Corbel 2009). Moreover, direct observational evidence for super-Eddington winds in ULXs is scarce (Walton et al. 2012, 2013; Middleton et al. 2014). Interestingly, a similar group of objects, such as S26 in NGC 7793 and MQ1 in M83, which do not appear to have luminous central X-ray sources, can none the less have more energetic optical bubbles (Pakull, Soria & Motch 2010; Soria et al. 2014) than classical ULXs. These two peculiar examples both appear to have radio jets (or at least hot spots) and relatively large cocoons. Such morphology resembles SS433, although the total energy content of the W50 bubble surrounding SS433 is two orders of magnitude lower (Pakull et al. 2010).

In the Galactic BH X-ray binaries, there is an observational anti-correlation between the presence of disc winds and jets. Winds are observed in soft or disc-dominated objects, and jets are typically seen (at lower Eddington rates) in hard-state objects (e.g. Ponti et al. 2012). Broadly speaking, in active galactic nuclei (AGNs), near-Eddington luminosities are also coupled with powerful winds, whereas relativistic jets tend to occur at lower accretion rates (e.g. King & Pounds 2015). The presence of a collimated jet structure in Holmberg II X-1 coupled with a high X-ray luminosity might be somewhat extraordinary if one assumes persistent near- or super-Eddington accretion. However, little is known about switching between sub- and super-Eddington accretion. Possibly the best examples for such transitions are the Galactic systems GRO J1655–40 (e.g. Meier 1996) and GRS1915+105 (e.g. Arai et al. 2009). Additionally, the higher BH masses inferred for sources like Holmberg II X-1 may imply longer characteristic time-scales (McHardy et al. 2006).

In summary, Holmberg II X-1 is a bona fide ULX with a typical X-ray luminosity of $\sim 10^{40}$ erg s^{-1} (e.g. Grisé et al. 2010). It is hosted by a nearby, relatively metal-poor (e.g. Prestwich et al. 2013) dwarf irregular galaxy at a distance of 3.39 Mpc (Karachentsev et al. 2002). It is associated with an optical (e.g. Kaaret, Ward & Zezas 2004) and a radio bubble (Miller, Mushotzky & Neff 2005). The optical environment is photoionized with an average isotropic X-ray luminosity of 4×10^{39} erg s^{-1} (Kaaret et al. 2004). The radio bubble is inflated due to jet activity, and the deduced average jet power of $Q_{\rm j} \sim 2 \times 10^{39}$ erg s^{-1} (Cseh et al. 2014) is comparable to the average X-ray luminosity. Its X-ray spectrum shows typical ULX features, like a soft excess and a spectral break (Kajava et al. 2012). Based on the energetics, the X-ray spectral properties, and the environment its mass is likely to be in the range of 25–100 $M_\odot$ (Goad et al. 2006; Cseh et al. 2014) with an accretion rate near or above the Eddington limit. The high accretion rate may also be supported by that the jet morphology indicates a recurrent activity (see below). Also, the above mass range might be supported by the longer activity of the source as compared to Galactic microquasars (Cseh et al. 2014).

How these massive stellar mass BHs evolve remains unclear. Early BH growth is often hypothesised to proceed via (intermittent) super-Eddington accretion (e.g. Pacucci & Ferrara 2015; Volonteri, Silk & Dubus 2015). To investigate if some ULXs and their observable properties can act as a proxy for super-Eddington BH growth in the early Universe, we present quasi-simultaneous and multi-epoch observations of the ULX Holmberg II X-1 (hereafter, Ho II X-1), which are summarized in Table 1. Our primary aim is to study the nature and evolution of the previously-detected central radio source (Cseh et al. 2014), and to investigate the link between the radio emission and the X-ray behaviour. In Section 2, we describe our observational results. In Section 3, we first discuss the X-ray spectra and the high-resolution radio properties of Ho II X-1, followed by our interpretation of the temporal evolution of the radio ejecta in Ho II X-1. Finally, we discuss the physical properties of the jet ejecta.

Table 1. Summary of the observations.

Instrument	Mode or configuration	Frequency or energy band	On-source time	Observation date
EVN	–	1.6 GHz	12.5 h	14 Jan 14
Swift	PC	0.3–10 keV	20.5 ks	17–22 Jan 14
EVN	–	5 GHz	12.5 h	28 Apr 14
Chandra	1/8	0.3–10 keV	11.8 ks	25 May 14
VLA	A	8–10 GHz	171 min	25 May 14

2 OBSERVATIONS, ANALYSIS, AND RESULTS

2.1 Joint *Swift*/XRT and EVN observations

2.1.1 Swift*/XRT observations*

The *Swift* X-ray telescope (XRT) observed Ho II X-1 (PI: Grisé) in photon counting (PC) mode on 17, 20, and 22 Jan 2014 starting from 13:36:59 UT, 00:48:59 UT, and 02:27:58 UT, for useful exposures of 5.71, 5.88, and 8.96 ks, respectively. We retrieved level 2 event files that were subjected to standard screening methods.[1] The source spectrum was extracted using an aperture of 20 pixels, which corresponds to 90 per cent of the PSF at 1.5 keV. The background was extracted using an aperture of radius 40 pixels, centred on a J2000 location of RA = 08:19:51.437 and Dec. = +70:47:46.29. The auxiliary response file (ARF) was created with XRTMKARF, which accounts for PSF correction.

After rebinning the spectrum to have a minimum of 30 counts per bin, we fit the X-ray spectrum using XSPEC v12.8.2 (Arnaud 1996) and a response matrix of swxpc0to12s6_20130101v014.rmf.[2] We fit the spectrum with an absorbed power-law model (TBABS*TBABS*POWERLAW) and froze the first hydrogen absorption column density to the Galactic value of $N_{\rm H} = 3.4 \times 10^{20}$ cm^{-2} (Dickey & Lockman 1990). We found a good fit of χ^2/d.o.f. = 0.99

[1] http://heasarc.nasa.gov/docs/swift/analysis/
[2] http://heasarc.gsfc.nasa.gov/docs/heasarc/caldb/data/swift/xrt/index.html

for 80 degrees of freedom (DoF), a photon index of $\Gamma = 1.91 \pm 0.08$, an equivalent hydrogen absorption column density of $N_{\rm H} = (5 \pm 2) \times 10^{20}$ cm^{-2}, and an unabsorbed flux of $(6.6 \pm 0.4) \times 10^{-12}$ erg cm^{-2} s^{-1} in the 0.3–10 keV energy range. The fitted power-law photon index of $\Gamma = 1.91$ is consistent with a hard X-ray spectrum. The flux corresponds to a luminosity of $(9.1 \pm 0.6) \times 10^{39}$ erg s^{-1} at the source distance of 3.39 Mpc (Karachentsev et al. 2002). We fit other models to the X-ray data. First, a disc blackbody model that gave a poor fit with a reduced $\chi^2 > 3$. A cutoff power-law model gave an adequate fit, but with a cutoff energy at 500 keV, indicating that a simple power-law fits well. A combination of a disc blackbody with a power law resulted a 0 keV inner disc temperature, indicating that a simple power-law fits well.

Motivated by the best-fitting model of Walton et al. (2015), we also fit the *Swift* spectrum with two disc blackbody models [TBABS*TBABS*(DISKBB+DISKBB)]. This fit resulted in a reduced χ^2/d.o.f. = 0.94 that may indicate an overconstrained model. The first hydrogen absorption column density was frozen to the Galactic value. The fit did not require any additional $N_{\rm H}$ on top of the Galactic one. The fit resulted in inner disc temperatures of $T_{\rm in,\,1} = 0.32 \pm 0.05$ keV and $T_{\rm in,2} = 1.7^{+0.3}_{-0.2}$ keV. The hotter component agrees within the errors with the result of Walton et al. (2015), and the cooler component is inconsistent within the errors; it is somewhat hotter than found by Walton et al. (2015).

2.1.2 *VLBI observations*

We carried out very long baseline interferometry (VLBI) observations of the central component of Ho II X-1 with the electronic European VLBI Network (e-EVN) under program codes EC045 and RC001 (PI: Cseh), at 1.6 and 5 GHz, respectively. The 1.6-GHz observation started on 14 January 2014 15:01:10 UT and had a total duration of about 18 h. The 5-GHz observation started on 28 April 2014 13:01:10 UT and lasted for about 18 h. At 1.6 GHz, the participating stations were Effelsberg (Ef; Germany), Jodrell Bank Lovell Telescope (Jb; UK), Medicina (Mc; Italy), Noto (Nt; Italy), Onsala (On; Sweden), Sheshan (Sh; China), Toruń (Tr; Poland), and Westerbork (Wb; the Netherlands). For the 5-GHz observation, the stations were Ef, Jb Mark II, Nt, On, Tr, Wb, Sh, and Yebes (Ys; Spain). The data recording rate was 1 Gbit s^{-1} per station (except Mc where it was 512 Mbit s^{-1}), and no data were received from Ys. There were eight subbands, each with 16 MHz bandwidth in both left and right circular polarization.

The observations were carried out in standard phase-referencing mode, using J0841+7053 as the phase–calibrator. The observations cycled continuously between the target and the reference source, spending 3.5 min on the target in every 5-min block. The data were calibrated in AIPS v31Dec12 (e.g. Greisen 2003) following standard procedures (Diamond 1995), and imaging was performed using DIFMAP (Shepherd, Pearson & Taylor 1994). Antenna-based gain correction factors were obtained from the phase calibrator after a global amplitude self-calibration step, which were fed back to AIPS and applied to the data. These corrections were typically less than 10 per cent at 1.6 GHz and less than 20 per cent at 5 GHz. Fringe-fitting was then repeated taking into account the clean component model of the calibrator.

At 5 GHz, we reached an rms noise level of 12 μJy beam^{-1}, the Gaussian restoring beam size was 2.7 × 2.1 mas, and we did not detect Ho II X-1. We set a 3-σ upper limit of 36 μJy on the flux density of the source.

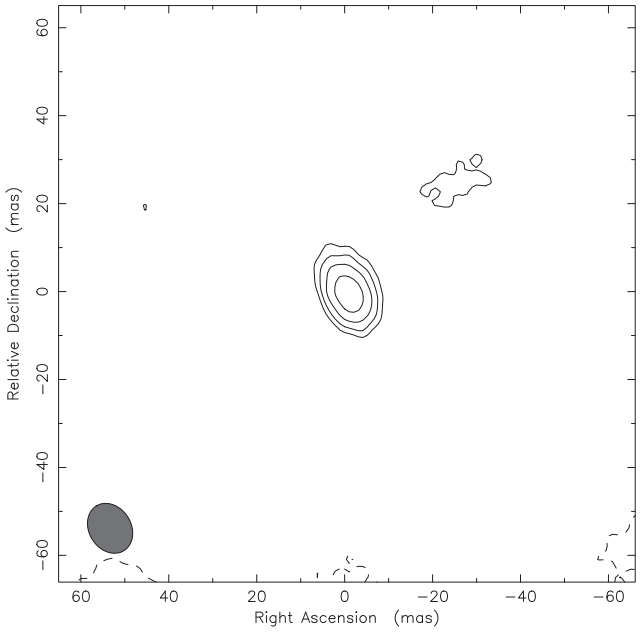

Figure 1. The 1.6-GHz e-EVN image of Ho II X-1 that was made using natural weighting. The lowest contours start at three times the rms noise level, at ±15 μJy beam^{-1}. Contours are increased by a factor of $\sqrt{2}$. The peak brightness is 53 μJy beam^{-1}. The Gaussian restoring beam size is 12 × 9.6 mas at a major axis position angle of 32°.

At 1.6 GHz, the rms noise level was ∼5 μJy beam^{-1}, and the Gaussian restoring beam size was 12 × 9.6 mas in PA 32°. Ho II X-1 was detected at a signal-to-noise ratio of >10 (Fig. 1), with a peak brightness of 53 μJy at a position of (J2000) RA = 08:19:28.9835 and Dec. = +70:42:18.9966 (accurate to within 1 mas). To check the compactness of the source, we fit the brightness distribution with a Gaussian in both the image and the visibility plane. Using the AIPS task JMFIT for the image-plane fit, we found a fitted peak brightness of 49 ± 6 μJy beam^{-1} and an integrated flux density of 84 ± 14 μJy. The integrated flux density is considerably higher than the peak brightness, likely indicating a resolved source.

A fit in the visibility plane using a point-source model in DIFMAP resulted in a total flux density[3] of $S_\nu = 65 \pm 6$ μJy. If we fit the source with a circular Gaussian model, we find a total flux density of $S_\nu = 88 \pm 11$ μJy and a full width at half-maximum (FWHM) size of 16.4 ± 1.7 mas. A comparison of these flux densities also indicates that the source is likely resolved. The obtained size of 16.4 ± 1.7 mas exceeds the restoring beam size of 12 × 9.6 mas. Furthermore, we estimate a resolution limit (Kovalev et al. 2005) of ∼3 mas that is well sampled by the image cell size of 1 mas.

To test at what angular resolution the source starts to be resolved, we produced an image with a restricted (u, v) range of 0–4 Mλ. The resulting image had a beam size of 33 × 30 mas. The source had a peak brightness of 67 μJy beam^{-1}, and a fit to a circular Gaussian model gave a total flux density of 95±10 μJy with a FWHM of 20 ± 1.6 mas. There is an apparent increase in all of the fit parameters although they are consistent with the above values within the errors. We conclude that the source is resolved on VLBI scales. We set a lower limit to its angular size of 16.4±1.7 mas that corresponds to a projected size of 0.26 ± 0.03 pc at a distance of

[3] The error on this and the subsequent flux densities includes a 5 per cent systematic uncertainty.

Table 2. Summary of results on the central component.

Instrument	Band	Flux density (μJy)	θ (mas)	T_b (K)
EVN	1.6 GHz	88 ± 11	16.4 ± 1.7	1.5×10^5
EVN	5 GHz	<36	–	–
VLA	8–10 GHz	12 ± 5	<235	–
Instrument	Band	Unabsorbed flux (erg cm^{-2} s^{-1})	Γ	N_H (cm^{-2})
Swift	0.3–10 keV	$(6.6 \pm 0.4) \times 10^{-12}$	1.91 ± 0.08	$(5 \pm 2) \times 10^{20}$
Chandra	0.3–10 keV	$(6.5 \pm 0.6) \times 10^{-12}$	1.88 ± 0.13	$(5 \pm 2) \times 10^{20}$

Note. The results of the Gaussian fits to the central radio component and the fit of an absorbed power-law model to the X-ray source. For the 1.6-GHz VLBI data, the brightness temperature (T_b) value is also provided.

Ho II X-1. A short summary is shown in Table 2. Should the true size be larger than 16.4 mas, we estimate an upper limit of ∼60 mas from our highest resolution VLA images.

2.2 Joint *Chandra* and VLA observations

2.2.1 Chandra *observations*

We observed Ho II X-1 with the *Chandra X-ray Observatory* under ObsID 15771 (PI: Jonker) using the Advanced CCD Imaging Spectroscopic array (ACIS) S3 chip in FAINT mode and with 1/8 subarray. The observation was carried out on 25 May 2014, started at 03:21:52 UT, and had a useful exposure of 11.85 ks. There were no strong background flares. The data were processed in a standard way, and we used the CIAO version 4.6 and the CALDB version 4.6.1 to further process the level 2 event files.

First, we checked for background flares following standard procedures.[4] We removed strong sources and then checked the extracted background light curve, and we found no strong flares during the observation. However, Ho II X-1 is a relatively bright X-ray source that caused a readout streak, which we therefore removed as described in the *Chandra* science thread pages.[5] Using WAVDETECT, we detected Ho II X-1 with a total of 6406 photons, and extracted its spectrum in the 0.3–10 keV range using SPECEXTRACT, with a circular aperture of radius 3 arcsec.

Given that we employed 1/8 subarray, providing a frame time of 0.4 sec, the expected[6] pileup fraction of Ho II X-1 is ∼5 per cent. To fit the spectrum, we used the SHERPA package and its built-in pile-up model, following the SHERPA thread pages.[7] First, we grouped our spectrum to have 30 counts per bin and then subtracted the background. We used an absorbed power-law model (XSTBABS*XSTBABS*XSPOWERLAW), setting the initial value of the hydrogen absorption column density to the Galactic one of $N_H = 3.4 \times 10^{20}$ cm^{-2}. We used the 'Neldermead' optimisation method to find a global solution that resulted in a reduced χ^2/d.o.f. of 1.14, a best-fitting value of the photon index of $\Gamma = 1.88 \pm 0.13$, and a hydrogen absorption column density of $N_H = (5 \pm 2) \times 10^{20}$ cm^{-2}. The resulting pile-up fraction was ∼6 per cent, in agreement with our estimate above.

To determine the flux, we fit the spectra without a pile-up model and froze the power-law index to $\Gamma = 1.88$. We found an unabsorbed flux of $(6.5 \pm 0.6) \times 10^{-12}$ erg cm^{-2} s^{-1} in the 0.3–10 keV range, corresponding to $L_X = (9.0 \pm 0.8) \times 10^{39}$ erg s^{-1} at the source distance of 3.39 Mpc. We also attempted to fit the same X-ray models to the *Chandra* spectrum as in Section 2.1.1. The spectrum is well fit by a power law and does not require any additional component. The power-law fit parameters and the X-ray luminosity are consistent with being the same for the *Swift* and the *Chandra* observations, which were separated by ∼4 months.

Following Walton et al. (2015), we fit the *Chandra* spectrum with two disc blackbody models in XSPEC [PILEUP*TBABS*TBABS*(DISKBB+DISKBB)]. We also fit a disc blackbody plus a p-free disc blackbody model [PILEUP*TBABS*TBABS*(DISKBB+DISKPBB)]. These fits resulted in a reduced χ^2/d.o.f. = 1.10 and 1.09, respectively. These reduced χ^2 values may indicate that employing two discs instead of a power law does not significantly improve the fit. The first hydrogen absorption column densities were frozen to the Galactic value. In both of the cases, the fit did not require any additional N_H on top of the Galactic one. The first fit resulted in inner disc temperatures of $T_{in,1} = 0.31 \pm 0.04$ keV and $T_{in,2} = 1.6^{+0.3}_{-0.2}$ keV. The second fit resulted in $T_{in,1} = 0.28 \pm 0.07$ keV, $T_{in,2} = 2.1^{+1.1}_{-0.7}$ keV, and $p = 0.6^{+0.3}_{-0.1}$ keV. The corresponding fitted temperatures between the first and the second fit agree within the errors. Furthermore, given that the value of p can be consistent with 0.75, with the standard disc, we cannot differentiate between a standard or a p-free disc model.

The fitted parameters of the first fit are consistent with being the same for the *Swift* and the *Chandra* observations. However, the cooler component is somewhat hotter than found by Walton et al. (2015). On the other hand, if a disc blackbody plus p-free disc are employed, both, the cooler and hotter component agrees within the errors with the result of Walton et al. (2015).

2.2.2 VLA observations

The Karl G. Jansky Very Large Array (VLA) observed Ho II X-1 simultaneously with *Chandra* on 25 May 2014. The observations were carried out under project code SF0330 and ran from 03:44:50 UT for a total of 3.5 h. The VLA was in its most-extended A-configuration, and the correlator integration time was 2 s. Two 1-GHz wide basebands covered the 8–10 GHz range (X band) with a total of 16 spectral windows, each with 64 2-MHz wide channels. We calibrated the data using CASA (McMullin et al. 2007) version

[4] http://cxc.harvard.edu/ciao/threads/filter_ltcrv/
[5] http://cxc.harvard.edu/ciao/threads/acisreadcorr/
[6] http://cxc.harvard.edu/toolkit/pimms.jsp
[7] http://cxc.harvard.edu/sherpa/threads/pileup/index.html

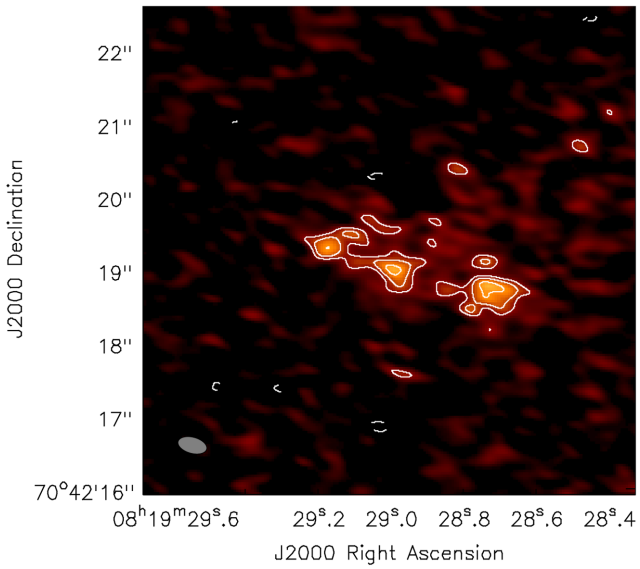

Figure 2. The VLA image of Ho II X-1 in X band, using Briggs robust = 1 weighting. The lowest contours start at three times the rms noise level, at ±6.6 μJy beam^{-1}. Contours are increased by a factors of $\sqrt{2}$. The peak brightness is 15 μJy beam^{-1}. The Gaussian restoring beam size is 0.41 × 0.22 arcsec at a major axis position angle of 75° E of N. The background colour image is arbitrarily scaled.

4.1.0 and the VLA pipeline version 1.2.0. The absolute amplitude and bandpass calibrator was 3C286, and the gain and phase calibrator was J0721+7120. The primary calibrator was observed once for 6 min, and the secondary calibrator was observed for 50 s in every 7.5-min block. The total on-source time was 171 min. There was no self-calibration applied. Images were made using Briggs robust = 1 and 0 weighting and the multifrequency synthesis (MFS) method with two Taylor terms. The rms noise was 2.2 μJy beam^{-1}, and the synthesized beam FWHM was 0.41 × 0.22 arsec in PA 75° (Fig. 2).

We detected three components, corresponding to those seen in C-band (4.5–6.5 GHz) VLA images (Cseh et al. 2014). The central, NE, and SW components were detected with a signal to noise ratio of 6.6, 6.0, and 6.8, respectively. The in-band spectral index of the components could not be constrained at these signal-to-noise ratios. We modelled these components with elliptical Gaussians using the JMFIT task within AIPS, and the results are shown in Table 3. We estimate the spectral index of the outer components between 5.24 and 9 GHz to be $\alpha_{\rm SW} = -0.5 \pm 0.4$ and $\alpha_{\rm NE} = -0.8 \pm 0.4$, where $S_\nu \propto \nu^\alpha$. However, we caution that the deconvolved size of the SW component is larger at X band than at C band. This could artificially flatten $\alpha_{\rm SW,}$ and the size of the components at X band are poorly constrained (Table 3).

For the central component, the size upper limits are in good agreement between the C-band uniformly-weighted image (<0.28 × 0.19 arsec) and the X-band robust 0 image (Table 3). Assuming a non-variable source, the spectral index of the central component is $\alpha_{\rm C} = -4.7 \pm 0.5$. We discuss possible interpretations for such a steep spectrum in Section 3.3. Note that the minimum baseline length in the X-band data was 10.5 kλ. To test whether resolution effects could be artificially steepening the spectrum, we produced a C-band image with a minimum baseline length of 10.5 kλ and found no change in either the peak brightness or the integrated flux density. This indicates that the unresolved central component at C band is unlikely to be contaminated by additional extended emission that was resolved out in our X-band observations.

3 DISCUSSION

3.1 Is Ho II X-1 in the canonical X-ray hard state?

It is common to fit ULX spectra with a two-component phenomenological model such as a power law and disc blackbody. On the other hand, high-quality *XMM-Newton* spectra of ULXs show a soft excess and a luminosity-dependent spectral break (Stobbart, Roberts & Wilms 2006; Gladstone, Roberts & Done 2009), and this is also the case for Ho II X-1 (Kajava et al. 2012), that may indicate super-Eddington accretion. On the other hand, Caballero-García & Fabian (2010) suggested that such a spectrum might be reflection-dominated and that the dominant contribution to the total luminosity is coming from the power-law component, potentially implying the sources to be sub-Eddington. However, in the case of Ho II X-1, this model resulted in a fitted photon index that might be too steep for a canonical hard state (Caballero-García & Fabian 2010). Furthermore, *NuSTAR* observations have confirmed the presence of a high-energy cutoff for a number of ULXs (Bachetti et al. 2013; Walton et al. 2014; Rana et al. 2015), which in those cases likely rules out a Compton hump arising from a reflection component in a canonical hard X-ray state. This has recently been shown specifically for Ho II X-1 (Walton et al. 2015).

Thus, despite the fact that the current spectra are well fit by a single power law, we argue that Ho II X-1 is unlikely to be in the canonical hard state. Additionally, there is no hint of a self-absorbed compact jet in Ho II X-1 (see later), as is typically seen in this state. It is also unlikely that Ho II X-1 is in a non-standard, efficient hard state (Rushton et al. 2010; Coriat et al. 2011) since the X-rays are steady and decorrelated from the radio emission. Also, our X-ray spectra may as well be fit with two disc blackbodies. In this case, it would be straightforward to exclude Ho II X-1 being in a canonical hard state, and such a fit possibly indicates a non-standard high state or a super-Eddington accretion state (Walton et al. 2015).

In the following, we investigate the temporal behaviour of the X-ray spectra. Grisé et al. (2010) presented multiple *Swift*/XRT observations of Ho II X-1, finding the source to remain in a soft spectral state for over four months in 2009/2010, in contrast to the

Table 3. The VLA X-band components.

Comp.	Peak (μJy b^{-1})	Flux dens. (μJy)	Size (mas × mas)	Robust	PA
Central	12 ± 3	12 ± 5	< 230 × 240	0	76°
Central	13 ± 2	50 ± 10	530 ± 170 × 480 ± 190	1	62°
SW	14 ± 2	64 ± 11	700 ± 140 × 450 ± 110	1	91°
NE	12 ± 2	35 ± 7	500 ± 160 × 300 ± 200	1	94°

Note. The Gaussian fit results of the different components.

hard spectra observed in 2006, which persisted for up to a month. The hard spectra from 2006 could also be fit with a disc blackbody and a power-law model. This is contrary to our spectra where this combination of models resulted in a 0 keV inner disc temperature. On the other hand, the power-law components are identical within uncertainties between these *Swift* data sets, so a variable soft component is likely to be present. Also, comparing our *Swift* and *Chandra* spectra, the power-law components are consistent with being the same even though they are separated by four months. Based on our observations, we conclude that the (apparently) hard spectra are in general steady, as compared to the soft spectra, which, beyond a possibly variable soft component, are associated with irregular flares (Grisé et al. 2010). The potential link between these flares and the radio activity needs further investigation.

3.2 VLBI morphology

In light of the relatively stable X-ray spectra, in the following, we shall investigate the contemporaneous behaviour of the central radio source that is coincident with the ULX position.

The 1.6-GHz VLBI component was found to be extended with a size of ∼0.26 pc. However, no milliarcsecond-scale radio emission was detected three months later at 5 GHz. This non-detection at 5 GHz is consistent with the extended morphology found at 1.6 GHz, and also with the optically thin synchrotron spectrum observed at lower resolution (Cseh et al. 2014). Thus, we infer that the VLBI emission is not due to a partially self-absorbed core jet. To estimate whether the source could be Doppler-boosted, we calculate its brightness temperature using:

$$\left(\frac{T_{\rm b}}{\rm K}\right) = 1.22 \times 10^6 (1+z) \left(\frac{S}{\mu\rm Jy}\right) \left(\frac{\rm GHz}{\nu}\right)^2 \left(\frac{\rm mas}{\theta}\right)^2. \quad (1)$$

After substituting $S_\nu = 88$ μJy at 1.66 GHz, $\theta = 16.4$ mas, and $z = 0.00079$, we find a brightness temperature of $T_{\rm b} \simeq 1.5 \times 10^5$ K. This is a relatively low value with respect to the equipartition value of relativistic compact jets of $T_{\rm b,\,eq} \simeq 5 \times 10^{10}$ K (Readhead 1994). Given that the Doppler-factor is $\delta \simeq T_{\rm b}/T_{\rm b,eq}$, the low $T_{\rm b}$ of the emission argues against Doppler-boosted emission and hence against relativistic beaming being responsible for strong radio variability (see next section).

3.3 Time-dependent radio behaviour

Assuming a non-variable source, the spectral index of the central component between 5.24 and 9.0 GHz is $\alpha_{\rm C} = -4.7 \pm 0.5$, which is significantly steeper than the previous estimate of $\alpha = -0.8 \pm 0.2$ (Cseh et al. 2014). In fact, such a steep spectrum is unphysical unless the synchrotron spectrum has a cutoff at the observed frequency due to e.g. synchrotron ageing. We investigate this option in the following section.

Since the two VLA measurements were taken about 1.5 yr apart, we therefore consider time variability. Taking the 5.24-GHz VLA peak brightness of 152 μJy beam^{-1} and a spectral index of $\alpha = -0.8 \pm 0.2$, the expected peak brightness of a point source at 9 GHz is 99 ± 11 μJy beam^{-1}. The detected X-band peak brightness of ∼12 μJy beam^{-1} is at least by a factor of 7.3 lower than this (a difference of $\sim 8\sigma$). Given that resolution effects were excluded (Section 2.2.2) and that the central source is point-like at both C and X band, this indicates that the flux density decreased with time.

3.4 The jet properties of Ho II X-1

The central component is due to optically thin synchrotron emission, consistent with a compact ejection. Since it was found to be a factor of ∼3 brighter than the outer components, this was interpreted as a renewed radio activity in the core (Cseh et al. 2014). The current VLA observation, obtained 1.5 yr later, also shows the same morphology. However, the brightness of the central component is comparable to or less than that of the outer components. Therefore, the central component has cooled much faster than the outer components. This is consistent with the deduced spectral indices in Section 2.2.2. The central component has apparently faded by at least a factor of 7.3, is resolved on VLBI scales, and is not affected by Doppler boosting.

The variation in the flux density over the course of ∼1.5 yr is likely a result of expansion. On the other hand, without a light curve, and with a VLBI component that is not (yet) resolved into a two-sided jet, the evolutionary stage of the ejection is unclear. Here, we assume a spreading jet and a Mach number similar to that of the large-scale jet (Cseh et al. 2014). Then a lateral expansion velocity of $0.2c$ is expected for a speed of c along the jet axis. This maximum expansion speed would result in a maximum radial increase of ∼4 mas (8 mas FWHM) over a year and may limit the age of the ejection to ≥2.1 yr. On the other hand, the bulk speed is unknown and based on the geometry it could be as slow as $0.17c$. Considering such a mildly relativistic bulk speed, the radial expansion rate would be ∼1.3 mas yr^{-1}, implying an increased ejection age of ∼13–46 yr for our measured size of 16.4–60 mas.

In the following, we deduce an approximate adiabatic time-scale ($t_{\rm ad}$) and compare it with the synchrotron cooling time-scale (τ). By assuming a fixed expansion speed of $v_{\rm exp} = 0.2c$, the adiabatic time-scale can be approximated from the apparent physical size (r) of the ejection using $t_{\rm ad} \simeq \frac{3}{2}\frac{r}{v_{\rm exp}}$. For an inner structure of size 16.4–60 mas, this gives $t_{\rm ad} \simeq 3.2$–11.7 yr. Next, we estimate the synchrotron lifetime of relativistic electrons at an observed frequency of 9 GHz, using $\tau \simeq 2.693 \times 10^{13} \nu^{-1/2} B^{-3/2}$ (e.g. Longair 1994), where the units are in Hz, mG, and yr. We estimate the magnetic field strength from minimum energy arguments, assuming equipartition between the energy in relativistic particles and that in the magnetic field. Using $B = 1.8 \times 10^7 \left(\frac{\eta L_\nu}{V}\right)^{2/7} \nu^{1/7}$ mG (e.g. Longair 1994), and substituting in the VLBI parameters of $\nu = 1.6 \times 10^9$ Hz, $V = 3 \times 10^{47}$ m^3, and $L_\nu = 1.21 \times 10^{17}$ WHz^{-1}, we find $B \simeq 0.77\eta^{2/7}$ mG, where $\eta - 1$ is the ratio of energy in protons to that in relativistic electrons. Here, we consider values of $\eta = 1$–100, and find $\tau \simeq (1.8$–$13) \times 10^3$ yr.[8] A comparison of these time-scales indicates that the ejection is dominated by adiabatic losses, which results in the observed rapid flux decay. The outer components are bright because they are likely the working surfaces where the jet ejecta interact with the surroundings, allowing the conversion of kinetic energy to radiation. Finally, we note that with an average jet power of $Q_{\rm j} \simeq 2.1 \times 10^{39}$ erg s^{-1}, the surrounding radio bubble might have been inflated in just ∼390 yr (Cseh et al. 2014).

3.5 Summary and implications

We have conducted quasi-contemporaneous X-ray and radio observations of Ho II X-1. The X-ray observations show steady, apparently hard spectra with properties that are identical to the power-law

[8] Here, we do not perform the calculations with the size upper limit of ∼60 mas because a higher size would mean even longer time-scales.

component observed in spectra from 2006 (Grisé et al. 2010). By contrast, other observations in 2009/2010 have shown soft spectra and irregular flaring activity (Grisé et al. 2010). Given the steady, apparently hard emission, the X-ray flux variability may well arise purely from the soft component. The VLBI data reveal an extended radio source with a size of 0.26 pc. Based on its variability and brightness temperature, we find that it is consistent with non-thermal emission and that it is not affected by Doppler boosting. This is consistent with a scenario where the radio emission is due to a jet ejection event. Assuming a laterally expanding jet, we estimate the dynamical age of the ejection to be $\geq$2.1 yr. Whether an ejection event could be correlated with the soft or flaring nature of the X-ray spectra remains to be investigated. On the other hand, we argue that the hard X-ray spectra are unlikely to correspond to a canonical hard state. This conclusion is also supported by the lack of a classical flat spectrum, partially self-absorbed compact radio jet. Also, the lack of any correlation between the X-rays and the radio emission may also rule out radiatively efficient hard states, i.e. the 'outlier branch' on the X-ray/radio correlation of BH X-ray binaries (e.g. Coriat et al. 2011). Using the VLA, we have detected a triple structure at 8–10 GHz that corresponds well to the morphology seen at lower frequencies. However, the central component has faded by at least a factor of 7.3 in just 1.5 yr. We explain the observed cooling with adiabatic expansion losses that dominate over synchrotron cooling, regardless of the jet composition (baryonic or leptonic).

Cseh et al. (2012) reported unresolved radio emission in the vicinity of the ULX IC 342 X-1 and concluded that it was inconsistent with a self-absorbed compact jet, and could instead be a clump of emission from the radio nebula. On the other hand, Marlowe et al. (2014) argued that this unresolved emission could be consistent with an expanded ejection similar to that in Ho II X-1. By comparison, it is indeed plausible that such a radio component in IC342 X-1 could have faded on a time-scale of a few years . If that is the case, then the quoted size limit on the ejection (Marlowe et al. 2014) of IC 342 X-1 might be too large because the spatial variation would be small even with highly relativistic expansion speeds.

In light of our results on Ho II X-1, it is possible that other ULX radio bubbles could also have been inflated by transient ejecta. This could imply that it is not necessary to invoke self-absorbed compact jets to inflate ULX bubbles. Moreover, the self-absorbed compact jet in Cyg X-1 has been argued to be incapable of inflating its bubble (Heinz 2006) due to the mismatch between the energetics of the jet and the bubble. On the other hand, expanding ejecta and disc winds, which are potentially triggered by high accretion-rate events, could serve as a more plausible explanation in the above cases, as they might indeed be capable of carrying the required energy.

Ho II X-1 shows a collimated jet structure that is coupled with a high average X-ray luminosity whose ionizing rate is comparable to the average jet power. This may be unexpected given that AGNs with high accretion rates show strong winds but no powerful jets (e.g. Gan et al. 2014; Tombesi et al. 2015). Similarly, in the context of regular BH X-ray binaries, the jet is also suppressed in disc-dominated states, and Meier (1996) argues that a super-Eddington wind could be a secondary jet suppression mechanism. None the less, Ho II X-1 does show discrete jet ejecta. This may imply that if the current X-ray luminosity is super-Eddington, then Ho II X-1 has to switch between sub- and super-Eddington rates to form jet ejecta. Alternatively, it could be that the source is not super-Eddington, but is rather in a persistent high, intermediate state where jet ejecta are thought to be released whenever crossing the so-called 'jet line'.

X-ray monitoring of the source with triggered radio observations could differentiate between any of the cases and test if X-ray flaring traces a jet ejection event.

ACKNOWLEDGEMENTS

DC thanks S. Thoudam for useful discussions. The National Radio Astronomy Observatory is a facility of the National Science Foundation operated under cooperative agreement by Associated Universities, Inc. The scientific results reported in this article are based in part on observations made by the *Chandra* X-ray Observatory. The EVN is a joint facility of European, Chinese, South African, and other radio astronomy institutes funded by their national research councils. JCAMJ is the recipient of an Australian Research Council Future Fellowship (FT140101082) and also acknowledges support from an Australian Research Council Discovery Grant (DP120102393). EK acknowledges fund from an NWO Vidi grant no. 2013/15390/EW. We acknowledge support from the Hungarian Scientific Research Fund (OTKA NN110333). SC acknowledges financial support from the UnivEarthS Labex program of Sorbonne Paris Cité (ANR-10-LABX-0023 and ANR-11-IDEX-0005-02).

REFERENCES

Arai A. et al., 2009, PASJ, 61, L1
Arnaud K. A., 1996, in Jacoby G. H., Barnes J., eds, ASP Conf. Ser.Vol. 101, Astronomical Data Analysis Software and Systems V. Astron. Soc. Pac., San Francisco, p. 17
Bachetti M. et al., 2013, ApJ, 778, 163
Bachetti M. et al., 2014, Nature, 514, 202
Belczynski K., Bulik T., Fryer C. L., Ruiter A., Valsecchi F., Vink J. S., Hurley J. R., 2010, ApJ, 714, 1217
Brorby M., Kaaret P., Feng H., 2015, MNRAS, 448, 3374
Caballero-García M. D., Fabian A. C., 2010, MNRAS, 402, 2559
Coriat M. et al., 2011, MNRAS, 414, 677
Crowther P. A., Barnard R., Carpano S., Clark J. S., Dhillon V. S., Pollock A. M. T., 2010, MNRAS, 403, L41
Cseh D. et al., 2012, ApJ, 749, 17
Cseh D. et al., 2014, MNRAS, 439, L1
Diamond P. J., 1995, in Zensus J. A., Diamond P. J., Napier P. J., eds, ASP Conf. Ser. Vol. 82, Very Long Baseline Interferometry and the VLBA. Astron. Soc. Pac., San Francisco, p. 227
Dickey J. M., Lockman F. J., 1990, ARA&A, 28, 215
Egorov O. V., Lozinskaya T. A., Moiseev A. V., 2013, MNRAS, 429, 1450
Farrell S. A., Webb N. A., Barret D., Godet O., Rodrigues J. M., 2009, Nature, 460, 73
Fender R. P., Homan J., Belloni T. M., 2009, MNRAS, 396, 1370
Feng H., Kaaret P., 2010, ApJ, 712, L169
Fryer C. L., 1999, ApJ, 522, 413
Gan Z., Yuan F., Ostriker J. P., Ciotti L., Novak G. S., 2014, ApJ, 789, 150
Gladstone J. C., Roberts T. P., Done C., 2009, MNRAS, 397, 1836
Goad M. R., Roberts T. P., Reeves J. N., Uttley P., 2006, MNRAS, 365, 191
Greisen E. W., 2003, in Heck A., ed., Information Handling in Astronomy – Historical Vistas. Kluwer, Dordrecht, 285, 109
Grisé F., Kaaret P., Feng H., Kajava J. J. E., Farrell S. A., 2010, ApJ, 724, L148
Grisé F., Kaaret P., Corbel S., Feng H., Cseh D., Tao L., 2012, ApJ, 745, 123
Heinz S., 2006, ApJ, 636, 316
Jonker P. G., Torres M. A. P., Fabian A. C., Heida M., Miniutti G., Pooley D., 2010, MNRAS, 407, 645
Kaaret P., Corbel S., 2009, ApJ, 697, 950
Kaaret P., Corbel S., Prestwich A. H., Zezas A., 2003, Science, 299, 365
Kaaret P., Ward M. J., Zezas A., 2004, MNRAS, 351, L83

Kajava J. J. E., Poutanen J., Farrell S. A., Grisé F., Kaaret P., 2012, MNRAS, 422, 990
Karachentsev I. D. et al., 2002, A&A, 383, 125
King A., Pounds K., 2015, preprint (arXiv:1503.05206)
Kovalev Y. Y. et al., 2005, AJ, 130, 2473
Lehmann I. et al., 2005, A&A, 431, 847
Liu J.-F., Bregman J. N., Bai Y., Justham S., Crowther P., 2013, Nature, 503, 500
Longair M. S., 1994, High Energy Astrophysics Volume2. Stars, the Galaxy and the Interstellar Medium, 2nd edn. Cambridge Univ. Press, Cambridge
McHardy I. M., Koerding E., Knigge C., Uttley P., Fender R. P., 2006, Nature, 444, 730
McMullin J. P., Waters B., Schiebel D., Young W., Golap K., 2007, in Shaw R. A., Hill F., Bell D. J., eds, ASP Conf. Ser. Vol. 376, Astronomical Data Analysis Software and Systems XVI. Astron. Soc. Pac., San Francisco, p. 127
Mapelli M., Bressan A., 2013, MNRAS, 430, 3120
Mapelli M., Colpi M., Zampieri L., 2009, MNRAS, 395, L71
Marlowe H. et al., 2014, MNRAS, 444, 642
McHardy I. M., Koerding E., Knigge C., Uttley P., Fender R. P., 2006, Nature, 444, 730
Meier D., 1996, ApJ, 459, 185
Mezcua M., Lobanov A. P., 2011, Astronomische Nachrichten, 332, 379
Mezcua M., Farrell S. A., Gladstone J. C., Lobanov A. P., 2013, MNRAS, 436, 1546
Mezcua M., Roberts T. P., Lobanov A. P., Sutton A. D., 2015, MNRAS, 448, 1893
Middleton M. J. et al., 2013, Nature, 493, 187
Middleton M. J., Walton D. J., Roberts T. P., Heil L., 2014, MNRAS, 438, L51
Miller N. A., Mushotzky R. F., Neff S. G., 2005, ApJ, 623, L109
Motch C., Pakull M. W., Soria R., Grisé F., Pietrzyński G., 2014, Nature, 514, 198
Pacucci F., Ferrara A., 2015, MNRAS, 448, 104
Pakull M. W., Grisé F., 2008, in Bandyopadhyay R. M., Wachter S., Gelino D., Gelino C. R., eds, AIP Conf. Ser. Vol. 1010, A Population Explosion: The Nature & Evolution of X-ray Binaries in Diverse Environments. Am. Inst. Phys., New York, p. 303
Pakull M. W., Mirioni L., 2002, preprint (arXiv:astro-ph/0202488)
Pakull M. W., Soria R., Motch C., 2010, Nature, 466, 209
Pasham D. R., Strohmayer T. E., Mushotzky R. F., 2014, Nature, 513, 74
Ponti G., Fender R. P., Begelman M. C., Dunn R. J. H., Neilsen J., Coriat M., 2012, MNRAS, 422, L11
Poutanen J., Lipunova G., Fabrika S., Butkevich A. G., Abolmasov P., 2007, MNRAS, 377, 1187
Poutanen J., Fabrika S., Valeev A. F., Sholukhova O., Greiner J., 2013, MNRAS, 432, 506
Prestwich A. H., Tsantaki M., Zezas A., Jackson F., Roberts T. P., Foltz R., Linden T., Kalogera V., 2013, ApJ, 769, 92
Rana V. et al., 2015, ApJ, 799, 121
Readhead A. C. S., 1994, ApJ, 426, 51
Rushton A., Spencer R., Fender R., Pooley G., 2010, A&A, 524, A29
Shepherd M. C., Pearson T. J., Taylor G. B., 1994, BAAS, 26, 987
Soria R., Long K. S., Blair W. P., Godfrey L., Kuntz K. D., Lenc E., Stockdale C., Winkler P. F., 2014, Science, 343, 1330
Stobbart A.-M., Roberts T. P., Wilms J., 2006, MNRAS, 368, 397
Tombesi F., Melendez M., Veilleux S., Reeves J. N., Gonzalez-Alfonso E., Reynolds C. S., 2015, Nature, 519, 436
van Dyk S. D., Sramek R. A., Weiler K. W., Hyman S. D., Virden R. E., 1994, ApJ, 425, L77
Volonteri M., Silk J., Dubus G., 2015, ApJ, 804, 148
Walton D. J., Miller J. M., Reis R. C., Fabian A. C., 2012, MNRAS, 426, 473
Walton D. J., Miller J. M., Harrison F. A., Fabian A. C., Roberts T. P., Middleton M. J., Reis R. C., 2013, ApJ, 773, L9
Walton D. J. et al., 2014, ApJ, 793, 21
Walton D. J. et al., 2015, ApJ, 806, 65
Webb N. et al., 2012, Science, 337, 554
Zampieri L., Roberts T. P., 2009, MNRAS, 400, 677

This paper has been typeset from a TEX/LATEX file prepared by the author.